Rock Mech. Rock Engng. (2001) 34 (3), 201–215

Rock Mechanics and Rock Engineering

Mechanical Response of Lined and Unlined Heated Drifts

By

D. Elsworth

Department of Energy and Geo-Environmental Engineering, Pennsylvania State University, University Park, PA, U.S.A.

Summary

Approximate relations are developed to determine the steady stresses and displacements that may develop in unlined and lined drifts heated above ambient, as representative of conditions in a nuclear waste repository. For a series of parallel, unlined drifts, radial convergence due solely to thermal effects is everywhere null at early-times; at late times it is a maximum inward at springline, and an equivalent maximum outward at crown and invert. Support pressures and hoop stresses are evaluated for a flexible liner placed in intimate contact with the drift wall, following excavation, where a full slip condition is applied at the drift-liner interface. For rock mass moduli of similar order to, or smaller than, the liner modulus, hoop stresses and support pressures are shown insensitive to rock mass parameters. Surprisingly, liner stresses are strongly controlled by liner modulus, liner Poisson ratio, liner thermal expansion coefficient, and instantaneous liner temperature, and only weakly by rock mass modulus. Response is shown independent of thermal expansion coefficient of the rock mass, and temperature distribution beyond the drift wall. The "misfit" expansion of the liner in the drift cavity controls liner stresses that rise linearly with the temperature of the liner, alone. Importantly, the results demonstrate the potential to control magnitudes of thermal stresses by the incorporation of compressible elements within the liner, or within the blocking or backfill behind the liner. Although the results are partly conditioned by the assumptions of a fully flexible liner and full slip conditions at the drift-liner interface, they serve to define the important parametric dependencies in the mechanical response of heated drifts.

1. Introduction

A variety of approaches have been applied to determine the stresses that develop in lined and unlined tunnels in response to excavation. These approaches include the linear elastic response of deep unlined circular section tunnels subject to hydrostatic or biaxial stress conditions (Kirsch, 1898 in Timoshenko, 1934; Savin, 1951; Terzaghi and Richart, 1952), shallow tunnels (Mindlin, 1940), and excavations of various geometries subject to plane strain conditions (e.g. Hoek and Brown, 1980). These analyses are useful to obtain rapid estimates of drift-wall stresses and displacements, and for the evaluation of zones of local instability that

may result from material failure at the drift wall, or interior, or on planes of weakness that may release key blocks (Elsworth, 1995; Yow, 1985). Local failures within the drift wall may change the excavation cross-section and redistribute stresses, requiring the use of numerical methods (e.g. Crouch, 1976; Eissa, 1980) to track stress changes until a stable excavation contour results (e.g. Ewy et al., 1987).

The underlying assumption that the drift-wall rocks behave elastically breaks down where stress to strength ratios are high, or where the mechanical response of the materials is either intrinsically nonlinear (e.g. Santarelli et al., 1986) or time dependent (Gnirk and Johnson, 1964). Where failure develops within the drift-wall, drift-local stress magnitudes are reduced as the load is shed away from the excavation (Ladanyi, 1974), and a stable profile may result. Where local failure occurs, the stresses developed within the drift wall rarely reach the magnitudes predicted by elastic theory (Burns and Richard, 1964; Hoeg, 1968; Muir Wood, 1975; Ranken et al., 1978; Einstein and Schwartz, 1979). The magnitude of induced stress is conditioned both by the choice of failure criterion (Brown et al., 1983) and the time of application of support (Ladanyi, 1974), and may be reasonably estimated if these parameters are known. These available solutions are for isothermal conditions, only.

Where large temperature changes are induced around tunnels and boreholes, the resulting thermal stresses may be significant. This is of some importance in defining breakdown pressures in hydraulic fracturing (Stevens and Voight, 1982), in defining the stability of petroleum wells (Perkins and Gonzales, 1981), and in the thermal fracturing of wells by the injection of quenching fluids (Murphy, 1979) in the development of hot dry rock geothermal reservoirs. In addition, the performance of lined and unlined drifts comprising a nuclear waste repository, such as that proposed in unsaturated tuffs at Yucca Mountain, Nevada (Department of Energy, 1998), is strongly linked to induced thermal stresses. One potential layout for the proposed repository will comprise a series of lined parallel drifts (Fig. 1),

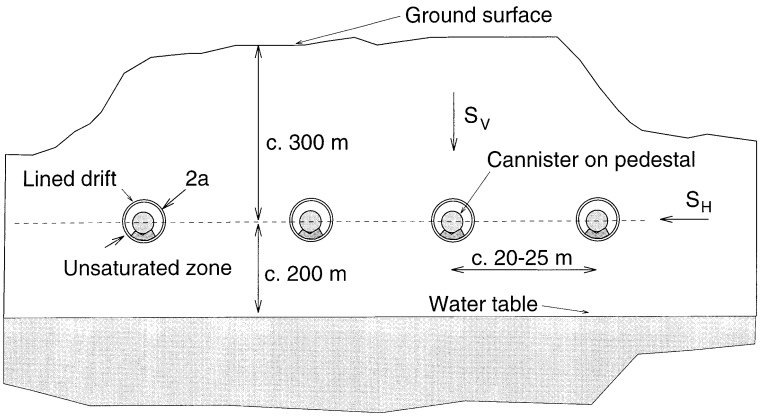

Fig. 1. Potential arrangement of drifts within a repository, typified by Yucca Mountain. Drift diameter is $2a$

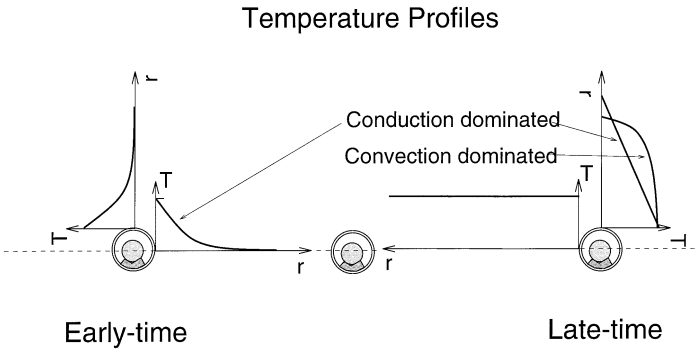

Fig. 2. Temperature distributions around drifts within a repository at both early-time (left), following introduction of the thermal source, and at late-time (right). The early-time temperature profile is radially symmetric before the aureoles of adjacent drifts overlap. At late time, temperatures are near constant in the horizontal direction, and decay linearly from the drift in the vertical direction. Where thermal transport is convection dominated, vertical temperature gradients close to the drift are reduced

each containing hot radioactive waste cannisters, that may result in wall temperatures of up to 180 °C. In this arrangement, the response of the composite liner-rock mass response is of interest, both in the short-term, and in the long-term. Distinction is made between these two temporal states, as the liner-rock interaction can be shown to change over time. Simple but robust approximations of the response are presented in this work to separately represent the early-time and long-term thermal behavior. In the early time, the transient thermal pulse from the drift wall decays rapidly with radius, as illustrated in Fig. 2; the thermal response of the drift is isolated from the other drifts, and thermal stresses and displacements are also largely independent of the adjacent drifts. In late time, the thermal aureoles of the individual drifts will have coalesced, and result in a zone of elevated temperatures that envelop the drift horizon (Fig. 2). Where thermal conduction dominates, temperatures will fall linearly with elevation above and below the horizontal drift axis, as shown in Fig. 2. Where the buoyant convection of water vapor from the drifts dominates response, the vertical thermal gradient will be flatter, and the temperature more homogeneous in the core of the drift horizon, as also shown in Fig. 2. For either conduction or convection dominated systems, the horizontal temperature gradient will be near zero. For these situations, the composite response of the entire drift horizon must be considered, including the presence of adjacent drifts. Approximate solutions are developed to represent these progressive responses in the following.

2. Drift Thermal Behavior

Thermal stresses may be evaluated if the evolving thermal region is defined. For the multiple drift geometry of Fig. 3, the simplest rigorous solution is to solve the thermal diffusion equation $\nabla^2 \cdot T = \kappa \partial T / \partial t$, where κ is thermal diffusivity, T is temperature, t is time and ∇ is the del operator $\partial^2/\partial x^2 + \partial^2/\partial y^2$, for Heaviside

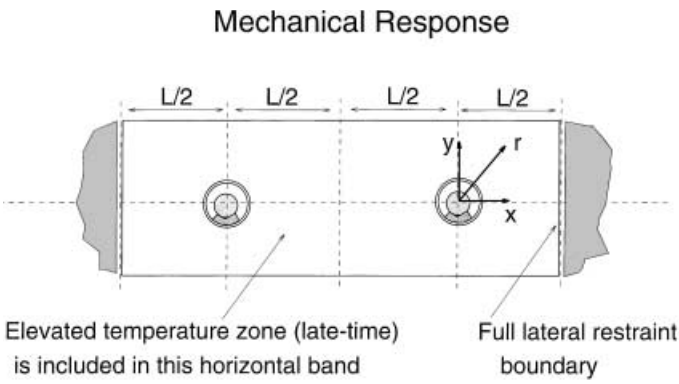

Fig. 3. Repeating geometry for multiple drifts at separation L between drift-centers. Mechanical boundary conditions are for full lateral restaint at $x = \pm L/2$. This current solution uses drifts cut into a thermally stressed horizontal band, constrained from lateral displacement throughout, prior to excavation

application of constant temperature boundary conditions on the repeating drift perimeter that returns to ambient as $y \rightarrow \pm\infty$. At early time, and close to the drift, this distribution approaches that for a solitary drift (Carslaw and Jaeger, 1959; Stevens and Voight, 1982) and is radially symmetric in the environs of each drift. At later times, and for multiple drifts, the distribution approaches a uniformly heated horizontal band, as represented in Fig. 3. Noted in the following is that for these end-member behaviors, the induced thermal stresses and displacements display some important and discernable patterns. This is the focus of the following, showing that the mechanical response is sensitive to the magnitude of induced drift-wall temperature, but insensitive to its interior distribution.

In this treatment, drift wall and liner stresses are evaluated by considering the behavior of a thin liner embedded within a circular-section drift. Adjacent parallel drifts are presumed sufficiently separated that mechanical interaction is minimal; this condition is typically met for drift separations greater than six radii (Bray, 1980; Brady and Brown, 1985). In the early-time, defined as the period before the zones of thermal influence overlap, the thermal response of any drift is not influenced by its neighbors. In this case, the thermal response is adequately represented by the behavior of a solitary drift (Fig. 2). At later times, the mutual interference of adjacent drifts cannot be ignored; mechanical interaction of the drifts remains inconsequential at all times for $L \geq 6a$; however, the thermal distribution loses its radial symmetry and develops a predominant horizontal spread. The multiple-drift response can be simplified by noting that the coalescing thermal aureoles produce a horizontal band of near-uniform elevated temperatures (Buschek, 1997) that in turn produce a zone of increased horizontal stress (Mack et al., 1989), as idealized in Fig. 3. If this unperforated horizontal band is restrained from displacing laterally, but unrestricted vertically, conditions of zero lateral strain will develop. If a single drift is subsequently excavated in this initially (laterally) restrained, horizontal band, the resulting thermally-induced hoop and radial stresses, and displacements may be determined. These results are exact for a single drift excavated

in a band that is initially restrained laterally, and approximate for multiple drifts that are sufficiently separated that their mechanical influence remains minimal ($L \geq 6a$). This arrangement enables the thermally-induced strains and displacements to be straightforwardly determined for the multiple drift geometry, and subsequently applied to determine the response of lined drifts.

2.1 Early-Time Response

The early-time response may be approximated by the behavior of a solitary drift in an infinite elastic medium, where the drifts are sufficiently separated that no mechanical or thermal interaction occurs. This solution is only valid until the thermal zones of adjacent drifts overlap, and the temperature distribution is no longer radially symmetric about each individual drift axis. The timing of this thermal transition is controlled by drift separation, relative to drift radius, and by thermal diffusivity of the rock mass. For any prospective repository at Yucca Mountain, drift centers would be separated by about 10 radii, and the early-time response would last for periods of one to a few years (Buschek, 1997; Nolting, 1997).

Consider a circular drift of radius, a, within an infinite medium represented by material coefficients representing coefficient of free thermal expansion, α_R, rock mass modulus, E_R and rock mass Poisson ratio, v_R, as illustrated in Fig. 4.

Substituting linear elastic constitutive equations into the radial equilibrium equation, and integrating, yields (Boley and Weiner, 1960; p. 289) the relevant displacement, u_r, radial stress, σ_{rr}, and tangential stress, $\sigma_{\theta\theta}$, relations with radius, r, and time, t, (Fig. 4) as:

$$u_r(r,t) = \frac{(1+v_1)\alpha_1}{r}\int_a^r Tr\,dr + C_1 r + \frac{C_2}{r}, \tag{1}$$

$$\sigma_{rr}(r,t) = \frac{\alpha_1 E_1}{r^2}\int_a^r Tr\,dr - \frac{E_1 C_1}{(1-v_1)} + \frac{E_1 C_2}{(1+v_1)r^2}. \tag{2}$$

and:

$$\sigma_{\theta\theta}(r,t) = -\frac{\alpha_1 E_1}{r^2}\int_a^r Tr\,dr + \alpha_1 E_1 T - \frac{E_1 C_1}{(1-v_1)} + \frac{E_1 C_2}{(1+v_1)r^2}, \tag{3}$$

where $E_1 = E_R/(1-v_R^2)$, $v_1 = v_R/(1-v_R)$ and $\alpha_1 = \alpha_R(1+v_R)$. E_1, v_1, and α_1 refer throughout to equivalent rock properties, and E_1^L, v_1^L, and α_1^L, introduced later, will refer exclusively to equivalent liner properties. The temperature at any location is defined as T, and the constants of integration, C_1 and C_2, must be determined from the mechanical boundary conditions. Requiring that temperatures return to ambient at infinity, and that displacements also vanish, by correspondingly setting $u_{rr}(r \to \infty, t) = 0$ in Eq. (1), defines $C_1 = 0$. Substituting $C_1 = 0$ into Eq. (2) and requiring that radial stresses vanish at the unlined drift wall, where $\sigma_{rr}(r = a, t) = 0$ also defines $C_2 = 0$. Resubstituting the null values of integration coefficients C_1 and C_2 into Eqs. (1) to (3) yields, for drift wall behavior:

$$u_r(r,t) = \frac{(1+\nu_1)\alpha_1}{r}\int_a^r Tr\,dr \quad \text{or} \quad u_r(a,t) = 0 \tag{4}$$

$$\sigma_{rr}(r,t) = \frac{\alpha_1 E_1}{r^2}\int_a^r Tr\,dr \quad \text{or} \quad \sigma_{rr}(a,t) = 0 \tag{5}$$

$$\sigma_{\theta\theta}(r,t) = -\frac{\alpha_1 E_1}{r^2}\int_a^r Tr\,dr + \alpha_1 E_1 T \quad \text{or} \quad \sigma_{\theta\theta}(a,t) = \alpha_1 E_1 T_L, \tag{6}$$

which for an upper integration limit of $r = a$, for the drift wall, and a drift wall temperature of $T(r = a, t) = T_L$, above ambient, yields zero displacement as $u_r|_{r=a} = 0$ and a drift wall stress of $\sigma_{\theta\theta}(r = a, t) = \alpha_R E_R T_L/(1 - \nu_R)$, invariant with time, and independent of the thermal distribution within the surrounding rock mass, provided it is radially symmetric. Stresses and strains are positive in compression. Surprisingly, for a single drift in an infinite medium, no convergence of the drift wall is expected (Murphy, 1979), regardless of the thermal loading history. If the long-term temperature distribution is uniform, as expected in the long term for a solitary drift, the hoop stresses and displacements would be unchanged; however, the interaction with adjacent drifts is not accommodated, and therefore must be treated in a different manner.

2.2 Late-Time Response

The late-time response may be represented by considering a horizontal band of near-uniform temperature above initial ambient, T, where mean horizontal displacements are restrained and vertical displacements are unconstrained. This is the geometry described in Fig. 3. The approach is to allow horizontal thermal stresses to build in this laterally-constrained horizontal band, as it is heated to a near-uniform temperature, T. Vertical thermal stresses will be null. If a single drift is then excavated, the exact stresses can be evaluated from well-known analytical solutions (Kirsch, 1898). This solution is exact for a solitary drift, present within a heated horizontal band where lateral displacements are fully restrained. It is approximate for multiple drifts, and will yield adequate results provided drift spacing is greater than about six drift-radii. In this instance it closely approximates the rigorous solution where lateral displacements are restrained, $u_x = 0$ at $x = \pm L/2$, as consistent with Fig. 3. Induced thermal-stresses may be readily evaluated for this constrained geometry, and used to directly evaluate thermal strains and thermal displacements.

2.2.1 Stresses

For a solitary circular tunnel under plane strain conditions, the radial $\sigma_{rr}(r)$ and tangential $\sigma_{\theta\theta}(r)$ stresses may be determined with radius, r, for the geometry of Fig. 3, as (Kirsch, 1898 in Timoshenko, 1934):

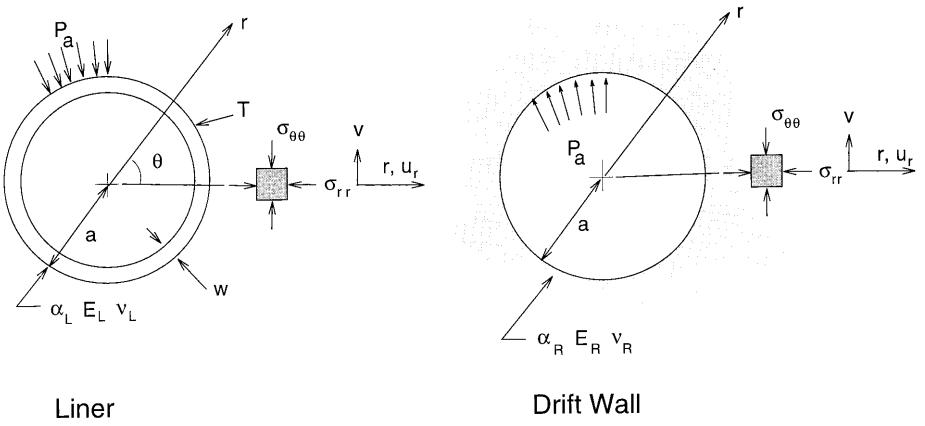

Fig. 4. Geometry of unlined drift and liner. Subscripts refer to liner (L) and rock mass (R) properties with regard to free thermal expansion coefficient, α, deformation modulus, E, and Poisson ratio, v. Temperatures are uniform within liner and drift wall, and of magnitude, T. The liner is of exterior radius, a, and fits tightly in the drift generating a thermal reaction pressure, P_a. Hoop ($\sigma_{\theta\theta}$) and radial (σ_{rr}) stresses are defined at any arbitrary radius, r, as are radial (u_r) and tangential (v) displacements

$$\sigma_{rr}(r) = \frac{1}{2}\left[(s_V + s_H)\left(1 - \frac{a^2}{r^2}\right) - (s_V - s_H)\left(1 - 4\frac{a^2}{r^2} + 3\frac{a^4}{r^4}\right)\cos 2\theta\right] \tag{7}$$

$$\sigma_{\theta\theta}(r) = \frac{1}{2}\left[(s_V + s_H)\left(1 + \frac{a^2}{r^2}\right) + (s_V - s_H)\left(1 + 3\frac{a^4}{r^4}\right)\cos 2\theta\right], \tag{8}$$

where s_V and s_H represent the vertical and horizontal far-field stresses and θ is the angle between the horizontal and the vector joining the drift center to the point of interest (Fig. 4). Provided the drifts are sufficiently separated, the induced stress fields will not be greatly affected. However, applying the requirement of null lateral strain prior to drift excavation, to represent mountain-scale restraint in the horizontal direction, enables the stresses around a heated drift to be directly determined. The horizontal stress, s_H, is augmented to $s_H + \alpha_1 E_1 T$, where T is the uniform temperature, relative to ambient. Thermally-induced stresses (superscripted by ΔT, below) may be evaluated from the difference between ambient and thermal states as:

$$\left\{ \begin{matrix} \sigma_{rr} \\ \sigma_{\theta\theta} \end{matrix} \right\}^{\Delta T} = \left\{ \begin{matrix} \sigma_{rr} \\ \sigma_{\theta\theta} \end{matrix} \right\}^{T} - \left\{ \begin{matrix} \sigma_{rr} \\ \sigma_{\theta\theta} \end{matrix} \right\}^{0}, \tag{9}$$

where ambient and thermal regimes are superscripted by 0 and T, respectively. Correspondingly, thermally induced stresses are:

$$\left\{ \begin{matrix} \sigma_{rr} \\ \sigma_{\theta\theta} \end{matrix} \right\}^{\Delta T} = \frac{1}{2}\alpha_1 E_1 T \left\{ \begin{matrix} \chi_r \\ \chi_\theta \end{matrix} \right\}, \tag{10}$$

where χ_r and χ_θ are derived from Eqs. (7) and (8), as noted in equations (A.1) and (A.2) in Appendix 1. These clearly satisfy a null change in radial stress at the unlined drift wall, that horizontal stress changes ($\sigma_{rr}^{\Delta T}(\theta = 0)$ and $\sigma_{\theta\theta}^{\Delta T}(\theta = \pi/2)$)

approach $\alpha_1 E_1 T$, and that vertical stresses ($\sigma_{\theta\theta}^{\Delta T}(\theta = 0)$ and $\sigma_{rr}^{\Delta T}(\theta = \pi/2)$) are unchanged as $r \to \infty$. At the boundary, thermally induced tangential stresses are periodic, and may be determined from Eq. (10) as:

$$\sigma_{\theta\theta}^{\Delta T}(r = a, t \to \infty) = \alpha_1 E_1 T[1 - 2\cos 2\theta], \tag{11}$$

and are invariant with time, since the drifts are enveloped in a region of uniform temperature, T, above ambient. This is assumed to be equivalent to the drift wall temperature.

2.2.2 Displacements

Radial (u_r) and tangential (v) displacements may be evaluated directly from radial (ε_{rr}) and tangential ($\varepsilon_{\theta\theta}$) strains, through integration. The inverse stress-strain relations for non-isothermal plane strain may be defined as (Boley and Weiner, 1960):

$$\left\{ \begin{array}{c} \varepsilon_{rr} \\ \varepsilon_{\theta\theta} \end{array} \right\}^{\Delta T} = \frac{1}{E_1} \left[\begin{array}{cc} 1 & -\nu_1 \\ -\nu_1 & 1 \end{array} \right] \left\{ \begin{array}{c} \sigma_{rr} \\ \sigma_{\theta\theta} \end{array} \right\}^{\Delta T} - \alpha_1 T \left\{ \begin{array}{c} 1 \\ 1 \end{array} \right\}. \tag{12}$$

The thermal strain field is then defined, for conditions on uniform temperature change from ambient of ΔT, as:

$$\varepsilon_{rr}^{\Delta T} = \alpha_1 T \frac{1}{2}[\chi_r - \nu_1 \chi_\theta - 2] \tag{13}$$

$$\varepsilon_{\theta\theta}^{\Delta T} = \alpha_1 T \frac{1}{2}[\chi_\theta - \nu_1 \chi_r - 2] \tag{14}$$

and these may be converted to displacements through integration of the strain-displacement relations, defined in radial coordinates as:

$$\varepsilon_{rr} = -\frac{du_r}{dr} \tag{15}$$

$$\varepsilon_{\theta\theta} = -\frac{u_r}{r} - \frac{du_\theta}{d\theta}. \tag{16}$$

Radial displacements may be determined by first integrating Eq. (15) to yield:

$$u_r = C_3 - \int \varepsilon_{rr}\, dr, \tag{17}$$

where C_3 is a constant of integration. Substituting Eq. (13) gives:

$$u_r = C_3 - \alpha_1 T \frac{1}{2}[\chi_{r,r} - \nu_1 \chi_{\theta,r} - 2r], \tag{18}$$

where the requirement that $u_r(r, \theta = 0) \to 0$ as $r \to \infty$, or $u_r(r, \theta = \pi/2) \to \alpha_1(1 + \nu_1)Tr$ as $r \to \infty$, defines $C_3 = 0$. Correspondingly, radial displacements around the drift are defined from Eq. (18), and the nondimensional convergence,

at $r = a$ is:

$$\frac{u_r}{a} = -\alpha_1 T 2 \cos 2\theta. \tag{19}$$

Of particular note is the periodicity, from springline to crown and invert, defining maximum convergence on the horizontal axis and maximum divergence, of equal magnitude, on the vertical axis. This conservation of the cross-sectional area of the drift is the equivalent of the null convergence anticipated for a solitary drift, apparent in Eq. (4). This null change in section, or drift circumference, is independent of the mechanical properties of the rock mass. Maximum convergence magnitudes are linked only to the coefficient of thermal expansion, and Poisson ratio, both typically defined within relatively narrow expected ranges. Convergence magnitudes are directly proportional to rock temperature, relative to ambient.

Tangential displacements may similarly be recovered by the integration of Eq. (16) to yield:

$$u_\theta = C_3 + C_4\theta - \int \varepsilon_{\theta\theta}\, d\theta - \int \frac{u_r}{r} d\theta, \tag{20}$$

where u_θ is a non-dimensional (angular) displacement and C_3 and C_4 are again constants of integration. The actual lineal displacement (units of length), v, is given as $v = ru_\theta$. The constants of integration, C_3 and C_4, are defined by noting from symmetry that $u_r(r, \theta = 0) = u_r(r, \theta = \pi/2) = 0$. Substituting Eqs. (14) and (18) into Eq. (20) and sequentially applying null drift-wall displacements for $\theta = 0$ and $\theta = \pi/2$ yields $C_3 = C_4 = 0$. This result may also be recovered by inspection, since both integrals are individually null over any full quadrant, from $\theta = 0 \rightarrow \pi/2$ or $\theta = \pi \rightarrow 3\pi/2$, for example. For the first integral, it is because tangential displacements must be zero at crown, invert and springline. The second integral is null over these limits because of the $\cos 2\theta$ periodicity of u_r, apparent in Eqs. (18) and (19). Correspondingly, tangential displacements are defined as:

$$u_\theta = -\alpha_1 T \frac{1}{2}\left[[\chi_{\theta,\theta} - \nu_1 \chi_{r,\theta} - 2\theta] - \frac{1}{r}[\chi_{r,r\theta} - \nu_1 \chi_{\theta,r\theta} - 2r\theta]\right]. \tag{21}$$

At the drift wall, $r = a$, and:

$$u_\theta = \alpha_1 T 2 \sin 2\theta \tag{22}$$

for the non-dimensional tangential displacement, and $v = ru_\theta$, to yield the actual lineal tangential displacement, v, as:

$$\frac{v}{a} = \alpha_1 T 2 \sin 2\theta, \tag{23}$$

that complements the periodicity of the drift wall convergence. Again, the magnitude of the tangential displacement is conditioned only by the coefficient of free thermal expansion of the rock mass and Poisson ratio, and is in direct proportion to the change in temperature.

3. Liner Thermal Behavior

A thin liner is assumed placed in intimate contact with the rock mass after initial excavation-induced displacements have occurred. From the foregoing analysis of tunnel convergence, the null change in circumference of the heated drift is noted, under both short-term and long-term conditions. If flexural rigidity of the liner is assumed to be small, and a full slip condition applied at the contact between the liner and the tunnel wall, the thermal loads applied to the liner may be approximately represented as radially symmetric. The response of a liner, of nominal radius, a, and thickness, w, as illustrated in Fig. 4, may be correspondingly determined from thin-wall theory. Under the assumption of a perfectly flexible liner, the resulting solution applies uniformly to early- and late-time response.

3.1 Thin-Walled Liner

For a thin-walled circular liner, subject to plane strain conditions, the radial displacement is conditioned by the drift reaction pressure, P_a, the liner-radius to thickness ratio, $M_L = a/w$, and the liner temperature above ambient, T, as:

$$\frac{u_r}{a} = M_L \frac{P_a}{E_1^L} - \alpha_1^L T, \tag{24}$$

where E_1^L and α_1^L now represent the equivalent liner properties [$E_1^L = E_L/(1-\nu_L^2)$, $\nu_1^L = \nu_L/(1-\nu_L), \alpha_1^L = \alpha_L(1+\nu_L)$], rather than those of the rock mass, as defined in Section 2.1. For the thin wall of the liner, the circumferential stress, $\sigma_{\theta\theta}$, is assumed to be of uniform magnitude, and is scaled by the liner-radius to thickness ratio, M_L, as:

$$\sigma_{\theta\theta} = M_L P_a. \tag{25}$$

3.2 Drift Reaction

With the displacement of the thin-walled liner defined relative to the uniformly applied drift reaction pressure, P_a, the response of the composite drift and liner may be evaluated. Where a uniform pressure of magnitude P_a is applied to the drift wall, the nondimensional displacement is:

$$-\frac{u_r}{a} = -\frac{P_a}{2G_R}\frac{a}{r}, \tag{26}$$

where G_R is the shear modulus of the rock mass, defined as $G_R = E_R/2(1+\nu_R)$.

3.3 Composite Drift Behavior

The expression representing radial displacement of a thin-walled liner (Eq. (24)) may be determined by equating the drift-wall and liner displacements as:

$$-\frac{u_r}{a} = \frac{P_a}{E_1^L} M_L - \alpha_1^L T. \tag{27}$$

Notably, the elastic and thermal constants, E_1^L and α_1^L, refer to liner materials, only, and M_L defines the liner geometry as $M_L = a/w$.

The uniform radial drift-liner reaction pressure, P_a, may be defined as:

$$P_a = \frac{\alpha_1^L T}{\frac{1}{2G_R} + \frac{M_L}{E_1^L}}, \tag{28}$$

where, perhaps surprisingly, the behavior is only weakly linked to rock mass parameters through the shear modulus, G_R. All other coefficients are for the liner materials.

The resulting mean liner circumferential stress, $\sigma_{\theta\theta}$, may be recovered from the drift-liner reaction pressure as:

$$\sigma_{\theta\theta} = M_L P_a. \tag{29}$$

Approximate relations may be recovered for the support pressure and hoop stress, where $M_L/E_1^L \gg 1/2G_R$, as:

$$P_a \approx \frac{\alpha_1^L E_1^L T}{M_L} \tag{30}$$

and:

$$\sigma_{\theta\theta} \approx \alpha_1^L E_1^L T. \tag{31}$$

This condition represents thin liners where the liner and rock moduli are of comparable magnitude, a situation commonly met in rock tunneling. These provide a full suite to define thermally induced stresses, subject to the assumptions of full slip and zero flexural rigidity.

4. Discussion and Results

Expressions (28) and (29) describe the response of a thin-walled liner. Surprisingly, reaction and hoop stresses are primarily conditioned by the thermal and elastic coefficients of the liner, α_L and E_L, and only mildly conditioned by rock mass shear modulus, G_R. Where rock mass modulus or the corresponding shear modulus, G_R, is of the same order as liner modulus, E_L, and drift diameter to liner thickness ratio, $M_L = a/w$, is large ($M_L > 10$), then $M_L/E_L \gg 1/2G_R$, and these relations may be approximated as:

$$P_a \approx \frac{\alpha_L E_L}{M_L(1 - \nu_L)} T \tag{32}$$

and:

$$\sigma_{\theta\theta} = M_L P_a \approx \frac{\alpha_L E_L}{(1 - \nu_L)} T, \tag{33}$$

where the subscripted L refers to liner properties. These expressions yield the important results that:

1. Thermal liner stresses, $\sigma_{\theta\theta}$, are controlled primarily by the effective liner properties of modulus, E_L, Poisson ratio, ν_L, thermal expansion coefficient, α_L, and liner thickness, w. These parameters are controllable, to some degree during design and fabrication, including the potential to provide compressible lagging or blocking, backfill, compressible joints, and the indeterminate influence of liner creep, and thereby control the magnitude of thermally induced stresses.
2. Perhaps surprisingly, there is only weak dependence on the rock mass deformation modulus and Poisson ratio. This is a direct consequence of the null aggregate displacement of the drift wall, the only influence being the stress reaction of the expanding liner ring against the drift wall. Where the liner is perfectly flexible, the periodic displacements induce no stresses within the liner. The only resulting stresses are the reaction against the drift wall due to thermal expansion of the liner.
3. Liner thermal stresses are surprisingly independent of the coefficient of thermal expansion of the rock mass, α_R, and depend only on the *instantaneous* liner temperature differential above ambient, T.

Representative data for Yucca Mountain (CRWMS, 1998) define mass moduli in the range 4–40 GPa, thermal expansion coefficients of the order $6–10 \times 10^{-6}/^{\circ}\mathrm{C}$, and sensible magnitudes of Poisson ratio of the order 0.2. Convergence estimates are defined proportional to $\alpha_R(1+\nu_R)T$ and, for a 5.5 m diameter drift, with a increase in temperature of 135 °C, are of the order of 14 mm. These are compared with numerical results obtained from FLAC, for drifts separated by 22.5 m, as documented in Table 1 (Nolting, 1997), which are in the range 8–11 mm. Notably, these are not influenced by modulus, and are of directly opposite sense in vertical divergence and horizontal convergence, as jointly predicted by Eq. (19). The slight mismatch between the analytical and numerical results, and the spread in values for the numerical results reflect a range of different initial stress states and mild material nonlinearities incorporated within the FLAC simulations, and not accommodated in the analytical solutions. The FLAC simulations use conditions of zero lateral displacement at $x = \pm L/2$, correctly representing the repeating

Table 1. Comparison of numerical results obtained from using FLAC (Nolting, 1997) with the solution developed in this paper (This work). Results are for unlined and lined drifts of diameter 5.5 m ($2a$) separated by 22.5 m (L). Rock properties are $E_R = 6$ GPa and 24 GPa, $\nu_R = 0.22$, and $\alpha_R = 8\ \mu\varepsilon/^{\circ}\mathrm{C}$. All results are for unlined drifts, except for the final evaluation of liner stresses. Properties of the 0.2 m thick (w) liner are $E_L = 27$ GPa, $\nu_R = 0.22$, and $\alpha_R = 10\ \mu\varepsilon/^{\circ}\mathrm{C}$. Temperature change is 135 °C

	FLAC results (Nolting, 1997)		This work	
	$E = 6$ GPa	$E = 24$ GPa	$E = 6$ GPa	$E = 24$ GPa
Vertical convergence (mm)	−8 to −10	−10	−14	
Horizontal convergence (mm)	+11	+10	+14	
Drift-wall hoop stress, crown (MPa)	18–26	60–70	24	96
Liner hoop stress, crown (MPa)	62	80	30	41

drift geometry. The analytical solution assumes a drift is cut into a horizontally stressed horizon (pre-mining zero lateral strain).

Thermally-induced stress magnitudes in the drift-wall may also be evaluated. The pre-mining stress magnitudes at a depth of 300 m are of the order 7 MPa vertical and 2.5 MPa horizontal (CRWMS, 1998). The post-excavation stresses are compressive at the springline, and near zero at the crown and invert. The addition of thermal stresses, after heating by 135 °C results in a switching of stress magnitudes to high compression in the crown and invert, and near zero at the springline. The resulting total crown and invert stresses are estimated to be of the order of 30–90 MPa, and are consistent with magnitudes evaluated from FLAC simulations (Nolting, 1997), defined in Table 1, that span 20–70 GPa. Notably the numerical results incorporate a modulus that varies with ambient stress level, hence a four-fold increase in initial rock modulus results in only a three-fold predicted increase in thermal stresses.

Where a concrete segmented liner is installed, with a comparable modulus to that of the rock, as $E_L = 27$ GPa, and with a comparable thermal expansion coefficient $\alpha_L = 10 \times 10^{-6}/^{\circ}\mathrm{C}$ to that of the rock mass, liner stresses may also be evaluated. For a liner thickness of 0.2 m and for rock mass moduli of 6 GPa and 24 GPa, the resulting hoop stresses are given in Table 1. As anticipated, these stress magnitudes are only slightly influenced by rock mass modulus. A four-fold increase in rock modulus only increases the stress magnitudes by about a third, confirming the expected diminished dependence of liner stresses on rock modulus. The numerical results incorporate friction between the liner and drift-wall, and therefore differ from the assumptions assumed in the solutions developed in this paper; hence the mismatch in results. Despite these differences, the overall correspondence between the numerical and analytical results suggests that the simplifying assumptions regarding non-interacting drifts, are indeed justified. The analytical solutions provide useful order-of-magnitude estimates of behavior.

These results underscore the relevance of the physical dependencies defined in the relatively straight-forward analytical solutions for unlined and lined drifts. Although the analysis is limited to a circular section drift within an infinite medium, and where liner bending stresses are neglected, the results are broadly applicable in defining the functional dependencies for other tunnel geometries.

Acknowledgments

This work was supported, in part, by the US Department of Energy through subcontract A10046 with TRW Environmental Safety Systems. This support is gratefully acknowledged. This acknowledgment does not constitute an endorsement of these results by the Department of Energy. Rick Nolting is thanked for supplying data on the detailed numerical analyses.

Appendix 1

The following coefficients may be defined directly from Eqs. (7) and (8). The root equations are:

$$\chi_r = \left(1 - \frac{a^2}{r^2}\right) + \left(1 - 4\frac{a^2}{r^2} + 3\frac{a^4}{r^4}\right)\cos 2\theta \tag{A.1}$$

$$\chi_\theta = \left(1 + \frac{a^2}{r^2}\right) - \left(1 + 3\frac{a^4}{r^4}\right)\cos 2\theta, \tag{A.2}$$

with the integrals of these relations defined in shorthand as $\int \chi_r\, dr = \chi_{r,r}$ for:

$$\int \chi_r\, dr = \left(r + \frac{a^2}{r}\right) + \left(r + 4\frac{a^2}{r} - \frac{a^4}{r^3}\right)\cos 2\theta = \chi_{r,r} \tag{A.3}$$

$$\int \chi_\theta\, dr = \left(r - \frac{a^2}{r}\right) - \left(r - \frac{a^4}{r^3}\right)\cos 2\theta = \chi_{\theta,r} \tag{A.4}$$

$$\int \chi_r\, d\theta = \left(1 - \frac{a^2}{r^2}\right)\theta + \left(1 - 4\frac{a^2}{r^2} + 3\frac{a^4}{r^4}\right)\frac{1}{2}\sin 2\theta = \chi_{r,\theta} \tag{A.5}$$

$$\int \chi_\theta\, d\theta = \left(1 + \frac{a^2}{r^2}\right)\theta - \left(1 + 3\frac{a^4}{r^4}\right)\frac{1}{2}\sin 2\theta = \chi_{\theta,\theta}, \tag{A.6}$$

where the constants of integration, C_3 etc., are omitted for clarity. The double integrals of these functions are defined as $\int\int \chi_r\, dr\, d\theta = \chi_{r,r\theta}$ for:

$$\int\int \chi_r\, dr\, d\theta = \left(r + \frac{a^2}{r}\right)\theta + \left(r + 4\frac{a^2}{r} - \frac{a^4}{r^3}\right)\frac{1}{2}\sin 2\theta = \chi_{r,r\theta} \tag{A.7}$$

$$\int\int \chi_\theta\, dr\, d\theta = \left(r - \frac{a^2}{r}\right)\theta - \left(r - \frac{a^4}{r^3}\right)\frac{1}{2}\sin 2\theta = \chi_{\theta,r\theta}, \tag{A.8}$$

where, again the constants of integration, of the form $C_3\theta + C_4$, are omitted for clarity, but incorporated where needed, such as in the solution of Eq. (20).

References

Boley, B. A., J. H. Weiner (1960): Theory of thermal stresses. Wiley, New York.

Brady, B. H. G., Brown, E. T. (1985): Rock mechanics for underground mining. Allen Unwin, Cambridge.

Bray, J. W. (1980): Personal communication.

Brown, E. T., Bray, J. W., Ladanyi, B., Hoek, E. (1983): Ground response curves for rock tunnels. J. Geotech. Engng. ASCE 109, 15–39.

Burns, J. Q., Richard, R. M. (1864): Attenuation of stresses for buried cylinders. Proc., Symp. on Soil-Structure Interaction, University of Arizona, Tucson, 378–392.

Buschek, T. (1997): Personal communication.

CRWMS M&O (1998): (Civilian radioactive waste management system, management and operation contractor), Cross drift geotechnical predictive report: geotechnical data report BABEA0000-01717-5700-00001 Rev. 01. Las Vegas, NV.

Crouch, S. L. (1976): The displacement discontinuity method. Int. J. Num. Meth. Engng. 10.

Department of Energy (1998): Viability assessment for a repository at Yucca Mountain, Nevada. Vol. 1–5, http://www.ymp.gov/va.htm.

Einstein, H. H., Schwartz, C. W. (1979): Simplified analysis for tunnel supports. J. Geotech. Engng. Div. ASCE 105, 499–518.

Elsworth, D. (1986): Wedge stability around a circular tunnel: Plane strain condition. Int. J. Rock Mech. Min. Sci. 23(2), 177–182.

Eissa, E. A. (1980): Stress analysis of underground excavations in isotropic and stratified rock using the boundary element method. Ph.D. Thesis, University of London, Vols. 1 and 2.

Ewy, R. T., Kemeny, J. M., Zheng, Z., Cook, N. G. W. (1987): Generation and analysis of stable excavation shapes under high rock stress. Proc., Int. Cong. of Int. Soc. Rock. Mech., Montreal, 875–881.

Gnirk, P. F., Johnson, R. E. (1964): The deformation behavior of a circular mine shaft situated in a viscoelastic medium under hydrostatic stress. Proc., 6th Symp. on Rock Mechanics, University of Missouri, Rolla, 231–259.

Hoeg, K. (1968): Stresses against underground structural cylinders. J. Soil Mech. and Foundations Div., ASCE 94, SM4, 833–858.

Hoek, E., Brown, E. T. (1980): Underground excavations in rock. Institution of Mining and Metallurgy, London.

Kirsch, G. (1898): Die Theorie der Elastizität und der Bedürfnisse der Festigkeitslehre. V.D.J. 42(29).

Ladanyi, B. (1974): Use of the long-term strength concept in the determination of ground pressure on tunnel linings. Proc., 3rd Int. Soc. Rock Mech., Denver, Vol. 2B, 1150–1156.

Mack, M. G., Brandshaug, T., Brady, B. H. G. (1989): Rock mass modification around a nuclear waste repository in welded tuff. NUREG/CR-5390.

Muir Wood, A. M. (1975): The circular tunnel in elastic ground. Geotechnique. 25(1), 115–127.

Mindlin, R. D. (1940): Stress distribution around a tunnel. Trans. ASCE 105, 1117–1140.

Murphy, H. D. (1979): Thermal stress cracking and the enhancement of heat extraction from fractured geothermal reservoirs. Geotherm. Energy Mag. 7(3), 22–29.

Nolting, R. (1997): Personal communication.

Perkins, T. K., Gonzales, J. A. (1981): Changes in earth stresses around a well bore caused by radially symmetrical pressure and temperature gradients. Paper SPE 10080, Proc., SPE 56th Ann. Tech. Conf. and Exhib., San Antonio, TX, Oct. 5–7.

Ranken, R. E., Ghaboussi, J., Hendron, A. J., Jr. (1978): Analysis of ground-liner interaction for tunnels. Report UTMA-IL-06-0043-78-3. Department of Transportation.

Santarelli, F. J., Brown, E. T., Maury, V. (1986): Analysis of borehole stresses using pressure-dependent, linear elasticity. Int. J. Rock Mech. Min. Sci. 23, 445–449.

Savin, G. N. (1951): Stress concentrations around holes. Pergamon Press, Oxford.

Stephens, G., Voight, B. (1982): Hydraulic fracturing theory for conditions of thermal stress. Int. J. Rock Mech. Min. Sci. Geomech. Abstr. 19, 279–284.

Terzaghi, K., Richart, F. E. (1952): Stresses in rock about cavities. Geotechnique 3, 57–90.

Timoshenko, S. (1934): Theory of elasticity. 1st edn., McGraw-Hill, New York.

Yow, J. L. (1985): Field investigation of keyblock stability. Ph.D. Thesis, University of California, Berkeley, and UCRL-53632, 227 pp.

Author's address: Derek Elsworth, Department of Energy and Geo-Environmental Engineering, Pennsylvania State University, University Park, PA 16802-5000, U.S.A.